JOURNAL OF VIROLOGY, Nov. 1991, p. 6015–6023
0022-538X/91/116015-09$02.00/0

Vol. 65, No. 11

Mechanisms of Receptor-Mediated Rhinovirus Neutralization Defined by Two Soluble Forms of ICAM-1

JEFFREY M. GREVE,* CARLA P. FORTE, CHRISTOPHER W. MARLOR, ANN M. MEYER, HELANA HOOVER-LITTY, DAVID WUNDERLICH, AND ALAN McCLELLAND

Molecular Therapeutics, Inc., Miles Research Center, 400 Morgan Lane, West Haven, Connecticut 06516

Received 23 May 1991/Accepted 15 August 1991

The majority of human rhinoviruses use intercellular adhesion molecule 1 (ICAM-1) as a cell surface receptor. Two soluble forms of ICAM-1, one corresponding to the entire extracellular portion [tICAM(453)] and one corresponding to the two N-terminal immunoglobulin-like domains [tICAM(185)], have been produced, and their effects on virus-receptor binding, virus infectivity, and virus integrity have been examined. Results from competitive binding experiments indicate that the virus binding site is largely contained within the two N-terminal domains of ICAM-1. Virus infectivity studies indicate that tICAM(185) prevents infection by direct competition for receptor binding sites on virus, while tICAM(453) prevents infection at concentrations 10-fold lower than that needed to inhibit binding and apparently acts at the entry or uncoating steps. Neutralization by both forms of soluble ICAM-1 requires continual presence of ICAM-1 during the infection and is largely reversible. Both forms of soluble ICAM-1 can alter rhinovirus to yield subviral noninfectious particles lacking the viral subunit VP4 and the RNA genome, thus mimicking virus uncoating in vivo, although this irreversible modification of rhinovirus is not the major mechanism of virus neutralization.

The majority of human rhinoviruses, the major causative agent of the common cold, utilize intercellular adhesion molecule 1 (ICAM-1) as a receptor on host cells (11). ICAM-1 is an integral membrane protein with a large N-terminal extracellular portion, a transmembrane anchor, and a short C-terminal cytoplasmic domain. The normal physiological function of ICAM-1 is to serve as a membrane-bound ligand of the leukocyte integrin lymphocyte function-associated antigen 1 (LFA-1) and mediate intercellular adhesion between leukocytes and a variety of cell types (17, 18, 33). The protein has sequence homology with members of the immunoglobulin supergene family, and its extracellular domain can be divided into five immunoglobulin-like domains (32, 35). Electron microscopy (34) has indicated that ICAM-1 is a highly elongated molecule.

The 3-dimensional structure of two rhinovirus serotypes have now been determined to atomic resolution by Rossmann and colleagues (15, 25). The virion is composed of a protein capsid of 60 protomeric units, consisting of the four protein subunits (VP1 to VP4), surrounding an RNA genome. Each of the 60 protomeric units possesses a recessed canyon that is likely to contain the receptor binding site (for a review, see reference 24). The dimensions of the canyon are such that it is too small to admit the combining site of an antibody but is apparently large enough to admit the virus binding site of ICAM-1. The precise extent of the virus binding site on ICAM-1 remains to be determined, although results from mouse-human chimeras and site-directed mutagenesis indicate that the N-terminal domain plays a major role in virus binding (20, 34), and a molecular model has been developed for the interaction of the N-terminal domain of ICAM-1 with the rhinovirus canyon (9). Detergent-solubilized transmembrane ICAM-1 binds to rhinovirus in solution (11), and a truncated form of ICAM-1 consisting of the extracellular domain binds to and neutralizes rhinovirus (19).

In an effort to further understand the molecular basis of rhinovirus–ICAM-1 interaction and to determine the mechanism by which soluble ICAM-1 neutralizes rhinovirus, we have produced two truncated soluble forms of ICAM-1. In this report, the properties of these proteins are described and their abilities to inhibit rhinovirus-receptor binding and infectivity are compared. These data indicate that there are three distinct mechanisms by which soluble ICAM-1 prevents virus infection and have implications for the role of the receptor in virus uncoating within host cells.

MATERIALS AND METHODS

cDNA constructions. Modified forms of the ICAM-1 cDNA were created by polymerase chain reaction (29) by using the full-length ICAM-1 cDNA pHRR-2 (11) as template. Plasmid DNA was digested with *Eco*R1 to excise the ICAM-1 insert and treated with alkaline phosphatase to prevent recircularization of the vector in subsequent ligation steps. Template DNA (10 ng) was subjected to 10 cycles of polymerase chain reaction amplification with the 5′ oligonucleotide primer GGAATTCAAGCTTCTCAGCCTCGCTATGGCTCCCAG CAGCCCCCGGCCC and the following 3′ oligonucleotide primers: GGAATTCCTGCAGTCACTCATACCGGGGGG AGAGCACATT for tICAM(453), TTCTAGAGGATCCTC AAAAGCTGTAGATGGTCACTGTCTG for tICAM(284), TTCTAGAGGATCCTCAAAAGGTCTGGAGCTGGTAGG GGG for tICAM(185), and TTCTAGAGGATCCTCACCGT TCTGGAGTCCAGTACACGG for tICAM(88). The polymerase chain reaction products were digested with either *Eco*R1 [tICAM(453)] or *Eco*R1 and *Bam*H1 [tICAM(284), tICAM(185), and tICAM(88)] and cloned into the polylinker site of Bluescript SK+ (Stratagene). Clones containing the desired inserts were verified by restriction analysis and DNA sequencing. The inserts were excised by digestion with *Hin*dIII and *Xba*I and inserted into the expression vector CDM8 (30).

Transfections and analysis of secreted proteins. For transient expression, COS cells were transfected by the DEAE-dextran method (16) and labeled 72 h after transfection with

* Corresponding author.

[^{35}S]cysteine in cysteine-free Dulbecco's modified essential medium (DMEM)–2% fetal calf serum for 18 h; culture supernatants were then immunoprecipitated with the anti-ICAM-1 monoclonal antibody c78.4 immunoglobulin G (IgG)-Sepharose and analyzed by sodium dodecyl sulfate-polyacrylamide gel electrophoresis (SDS-PAGE) as described previously (11). Stable CHO transfectants were obtained by cotransfection of ICAM-1 cDNAs with pSV2-dihydrofolate reductase into dihydrofolate reductase-deficient CHO cells by the calcium phosphate method or by electroporation (3). Transfected cells were cloned, and individual clones secreting ICAM-1 protein were identified by radioimmunoassay (RIA) of culture supernatants. Cell lines secreting tICAM(453) (CT.2A) and tICAM(185) (CD12.1A) were selected for further study and were subjected to gene amplification in methotrexate-containing media (3). A clone derived from CT.2A (resistant to 100 nM methotrexate) and a clone derived from CD12.1A (resistant to 1 μM methotrexate) were used for purification of soluble truncated proteins.

RIA. Two monoclonal antibodies, c92.5 (which recognizes the same epitope as c78.4) and c78.5, define two distinct conformational epitopes on ICAM-1 (20). These two antibodies were utilized in an RIA for soluble ICAM-1. c92.5 IgG was absorbed onto Immulon-1 (Dynatech, Inc.) microtiter plates, the plates were blocked by treatment with a solution of 10 mg of bovine serum albumin (BSA) per ml–N buffer (10 mM HEPES [*N*-2-hydroxyethylpiperazine-*N*′-2-ethanesulfonic acid]–200 mM NaCl–1 mM $CaCl_2$–1 mM $MgCl_2$ [pH 7.5]), and the plates were incubated with ICAM-1-containing samples. The plates were then washed with N buffer–0.05% Tween 20 and incubated with ^{125}I-c78.5 IgG (labeled with ^{125}I-Bolton-Hunter reagent), and the bound radioactivity was determined after the plates were washed and the radioactivity was solubilized with 1% SDS. The concentration of truncated ICAM-1 was determined by comparison with a standard curve of purified ICAM-1.

Protein purification. ICAM-1 was prepared from detergent lysates of HE1 cells, and tICAM(453) and tICAM(185) were purified from culture supernatants of their respective CHO transfectant cell lines by monoclonal antibody affinity chromatography as described previously (11) and then by either ion-exchange chromatography on Mono-Q for tICAM(453) with absorption in 10 mM Tris (pH 6.0) and elution with a 0 to 0.5 M NaCl gradient or gel filtration on Superose-12 columns (Pharmacia) for tICAM(185). Protein concentration was quantitated by amino acid analysis and by RIA. Amino acid analysis was performed on an Applied Biosystems model 420A amino acid analyzer.

Hydrodynamic properties. The f_{exp}/f_0 values for truncated ICAM-1 proteins were determined from the apparent Stokes' radii (R_S) determined by gel filtration on a Superose-12 column calibrated with protein standards (ferritin, 61.0 nm; catalase, 52.2 nm; bovine serum albumin, 35.5 nm; ovalbumin, 30.5 nm; and RNase A, 16.4 nm) and the calculated molecular weights of the core-glycosylated form of the proteins (determined by SDS-PAGE synthesized in the presence of swainsonin), as follows: $f_{exp} = 6\pi\eta R_S$ and $f_0 = (v_2 + \delta v_1^0/v_2)^{1/3} f_{min}$ (frictional coefficient of solvated sphere), where $f_{min} = 6\pi\eta(3Mv_2/4\pi N_0)^{1/3}$ (frictional coefficient of an unsolvated sphere). The following values are assumed: $v_2 = 0.73$ cm^3/g (partial specific volume of protein), $v_1^0 = 1.0$ cm^3/g (partial specific volume of solvent), $\delta = 0.35$ g of H_2O per g of protein (solvation of protein), $\eta = 0.01$ g/(cm · s) (viscosity of solvent), and $v_1^0 = 1.0$ cm^3/g (specific volume of the solvent). The molecular weights of tICAM (453) and tICAM(185) were assumed to be 64,100 and 27,200, respectively.

CD. Circular dichroism (CD) spectra were recorded on an AVIV model 62DS spectrometer. Protein solutions at approximately 0.5 mg/ml in the indicated buffers were scanned at 20°C in a cell with a 0.1-cm path length. Five repetitive scans (1-nm interval, 1.5-nm bandwidth) were averaged, buffer-subtracted, and then smoothed for each spectrum. Molar ellipticity was calculated by using protein concentrations determined by amino acid analysis. The spectra for c92.5 IgG, tICAM(453), and tICAM(185) were collected in 20 mM sodium phosphate buffer (pH 7.5), and the spectrum for ICAM-1 was collected in 0.1% octylglucoside–150 mM NaCl–10 mM sodium phosphate (pH 7.5).

Virus binding assay. ICAM-1 (100 ng), purified as described previously (11) in the presence of 0.1% beta-octylglucoside, was absorbed to Immulon-4 (Dynatech) microtiter plates by 10-fold dilution into N buffer, and the plates were incubated overnight at 4°C. The ICAM-1-coated plates were washed, blocked with a solution of 10 mg of BSA-N buffer per ml, and then washed extensively with 0.1% Triton X-100–N buffer–1 mg BSA per ml. The absorbed ICAM-1 was stably bound under these conditions and supported the binding of ^{35}S-HRV3. ^{35}S-HRV3 (2×10^5 cpm/ml) was preincubated with various amounts of ICAM-1 proteins for 30 min at 34°C. A 0.1-ml portion of these samples was added to the wells of the ICAM-1-coated microtiter dish and then incubated for 3 h at 34°C. The plates were washed extensively, and the bound radioactivity was solubilized with 1% SDS and quantitated by scintillation counting; maximum binding ranged between 20 and 25% of input virus.

Virus growth and infectivity assays. Human rhinovirus type 3 (HRV3) was used as a prototype of a major receptor rhinovirus throughout this study because it has a higher affinity toward receptor than the more commonly used serotype, HRV14 (10). HRV3 (obtained from the American Type Culture Collection) and [^{35}S]methionine-labeled HRV3 were propagated in HeLa S3 cells and purified as described previously (11). [^{3}H]uridine-labeled HRV3 was prepared in the same manner as [^{35}S]methionine-labeled HRV3, except that infected cells were labeled in DMEM–2% fetal calf serum containing 1 μg of actinomycin C_1 and 100 μCi of [^{3}H]uridine per ml (Amersham). All infectivity assays were performed with HeLa S3 cells in DMEM–2% fetal calf serum. Viral plaque assays were performed by incubating various dilutions of HRV3 with monolayers of HeLa cells in 35-mm-diameter cluster wells (Costar) for 30 min at 34°C in a volume of 1 ml. The monolayers were then washed and overlayed with 0.5% agarose (SeaPlaque; FMC Corp.) in DMEM–2% fetal calf serum, and plaques were scored after 2 to 3 days of incubation at 34°C following staining with crystal violet (21). For measurement of infectivity at high multiplicity of infection (MOI) (see Fig. 3C), 0.1 ml of HRV3 at 10^7 PFU/ml was preincubated with various concentrations of soluble ICAM-1 for 30 min at 34°C and then added to wells of a 96-well microtiter dish containing 10^4 HeLa cells per well. The cultures were then scored after a single cycle of virus replication by staining with crystal violet (22) at 24 h postinfection and determining the optical density at 550 nm on a plate reader (Molecular Devices). All experiments were performed in triplicate, and the results were expressed as the concentration of ICAM-1 needed to reduce the optical density at 550 nm by 50%. Specific infectivity (PFU/cpm) was determined by plaque assay from the peak fractions of clearly resolved 149S, 135S, and 80S species.

Sedimentation analysis of rhinovirus. Samples in 0.1 ml

were sedimented through 5 ml of 5 to 25% sucrose gradients (in N buffer–1 mg of BSA per ml) at 225,000 × *g* in an SW50.1 rotor for 45 min at 4°C. Gradients were fractionated from the bottom into approximately 20 fractions. Apparent S values were determined by the rate of sedimentation relative to standards (catalase, 11.3S; glutamate dehydrogenase, 22.6S; and rhinovirus, 149S).

Dot blot analysis of viral RNA. Peak fractions from a sucrose gradient were precipitated with 7% polyethylene glycol–0.6 M NaCl (21), and the pellets were resuspended in 0.1 ml of 1% SDS. RNase-free glycogen (Boehringer Mannheim) was added as a carrier to a concentration of 200 μg/ml, and RNA was extracted essentially as described by Rueckert and Pallansch (27) from equal amounts of [^{35}S]methionine radioactivity (2,500 cpm, or approximately 10 ng of HRV3). Samples were applied to Gene Screen Plus filters (NEN) in dot blot apparatus as described previously (31). Filters were then prehybridized with 2× SSC (1× SSC is 0.15 M NaCl plus 0.015 M sodium citrate)–5× Denhardt's solution–0.5% SDS–0.2 mg of salmon sperm DNA per ml for 1 h at 37°C and then hybridized with a γ-^{32}P-labeled oligonucleotide probe for nucleotides 455 to 471 of the positive (+) strand of HRV14 (5′-GCATTCAGGGGCCGGAG-3′; final concentration of 2 ng/ml) for 18 h at 37°C. The blot was washed with 2× SSC–1% SDS twice at 20°C and twice at 42°C before autoradiography.

RESULTS

Expression of soluble truncated forms of ICAM-1. ICAM-1 cDNAs encoding soluble proteins were constructed by inserting stop codons within the reading frame of the ICAM-1 polypeptide. Thus, stop codons were inserted immediately before the first residue of the transmembrane domain, at the predicted ends of domains 1, 2, and 3, domains 1 and 2, and domain 1 to produce a series of progressively truncated proteins (Fig. 1A). The cDNAs were cloned into the expression vector CDM8, transfected into COS cells for transient expression, and cotransfected with pSV2-dihydrofolate reductase into CHO cells for establishment of stable cell lines. In the experiment for which the results are shown in Fig. 1B, the secretion of various forms of truncated ICAM-1 in transiently transfected COS cells was examined. The results indicated that the entire extracellular domain, tICAM(453), and the two N-terminal domains, tICAM(185), were efficiently secreted from transfected COS cells as species of 80,000 Da and 43,000 Da, respectively (Fig. 1B). The level of expression of domains 1, 2, and 3 [tICAM(283)] was approximately 10-fold lower than those of the above-mentioned fragments, and the secreted protein was more heterogeneous in mobility on SDS-PAGE. Expression of domain 1 [tICAM(88)] could not be detected in COS cells, and alternative constructs in which the stop codon was shifted to several sites N or C terminal to residue 88 also failed to produce detectable amounts of protein. In order to obtain sufficient quantities of protein for functional and structural studies, CHO cell transfectants were prepared, cloned, and subjected to stepwise gene amplification in increasing concentrations of methotrexate. This resulted in the derivation of cell lines secreting 1.5 μg of tICAM(453) and 1.0 μg of tICAM(185) per ml. A stable cell line expressing tICAM(283) was not obtained, perhaps because the low level of secretion was at the limit of sensitivity of the immunoassay. The cells were adapted to serum-free media, and the secreted ICAM-1 proteins were purified to homogeneity from culture supernatants (Fig. 1C).

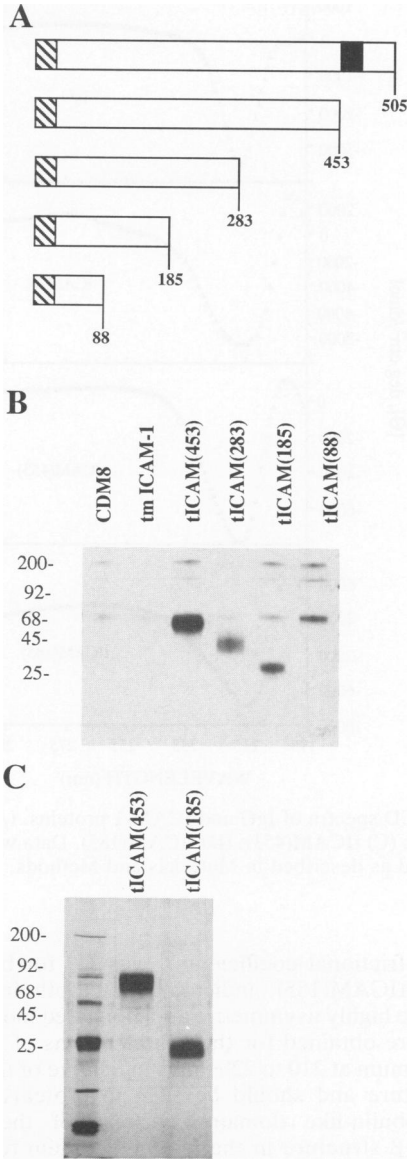

FIG. 1. Secretion of soluble ICAM-1 proteins. (A) Diagram of progressively truncated forms of ICAM-1 used in transfection experiments. The crosshatched section indicates signal sequence, and the filled section indicates the transmembrane region. (B) Fluorograph of [^{35}S]cysteine-labeled products secreted by COS cells analyzed by SDS-PAGE. The loading of lanes containing tICAM(283) and tICAM(88) is 10-fold higher than the loading of other lanes. (C) Silver-stained gel of purified tICAM(453) and tICAM(185) produced by CHO cell transfectants. In panels B and C, molecular weight markers (in thousands) are indicated on the left.

Several of the physical properties of tICAM(453) and tICAM(185) were examined. Both proteins were quantitatively immunoprecipitated by two monoclonal antibodies, c78.4 and c78.5, directed against two distinct conformation-dependent epitopes on ICAM-1 (data now shown), indicating that these epitopes were contained within the first two domains and providing evidence that the purified proteins were correctly folded. The Stokes radii of tICAM(453) and tICAM(185) were 5.3 and 3.9 nm, respectively, and the frictional ratio, f/f_0 (the ratio between the observed and

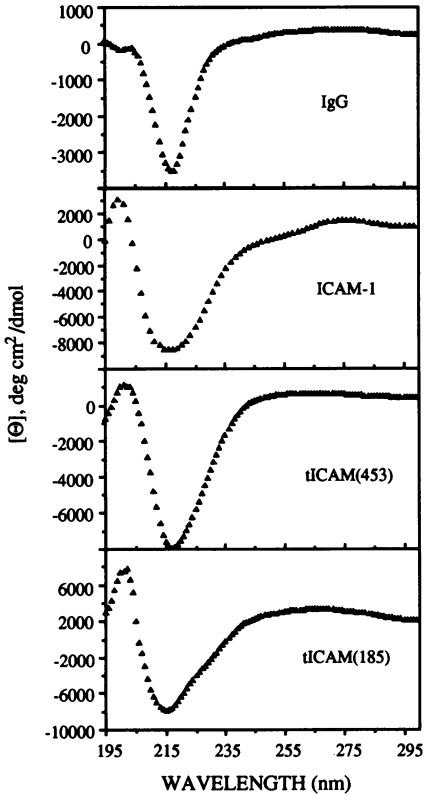

FIG. 2. CD spectra of IgG and ICAM-1 proteins. (A) c92.5 IgG; (B) ICAM-1; (C) tICAM(453); (D) tICAM(185). Data were collected and analyzed as described in Materials and Methods.

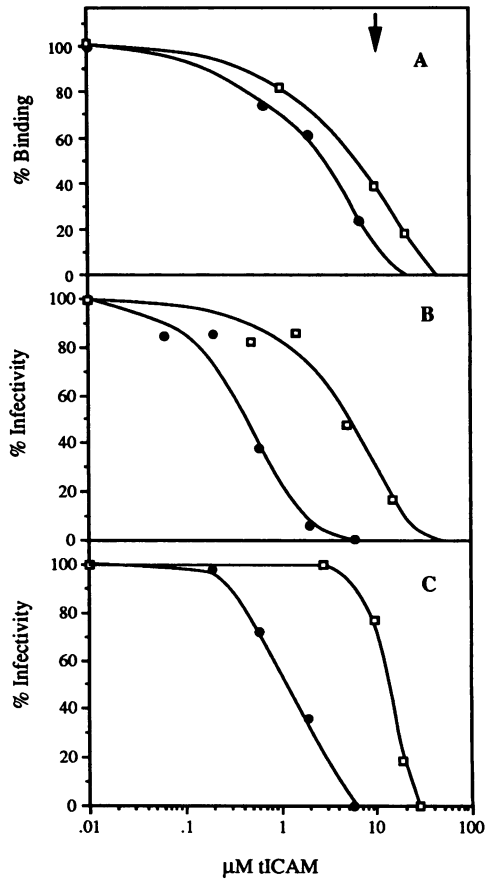

FIG. 3. Inhibition of virus binding and virus infectivity by soluble forms of ICAM-1. (A) ^{35}S-HRV3 was preincubated with various concentrations of soluble ICAM-1 for 30 min at 34°C, and binding to immobilized ICAM-1 was determined as described in Materials and Methods. (B) Reduction in virus titer by soluble ICAM-1. Approximately 2×10^2 PFU of HRV3 was preincubated with soluble ICAM-1 in 1 ml, and virus titer was determined by plaque assay as described in Materials and Methods. (C) Inhibition of virus infectivity under conditions of the virus-binding assay. HRV3 at 10^7 PFU/ml was preincubated with various concentrations of soluble ICAM-1 used to infect HeLa cells in a single-cycle, high-MOI infection (MOI, 100). Infectivity was determined after 24 h as described in Materials and Methods. tICAM(453), solid circles; tICAM(185), open squares. Arrow indicates the concentration of ICAM-1 at which the data shown in Fig. 4 were obtained.

calculated frictional coefficients), was 1.9 for both tICAM (453) and tICAM(185), indicating that both fragments of ICAM-1 are highly asymmetric and elongated molecules. CD spectra were obtained for the soluble forms of ICAM-1. A single minimum at 210 to 220 nm is indicative of the presence of β structure and should be seen in proteins containing immunoglobulin-like domains because of the extensive amount of β structure in the immunoglobulin fold (38). As internal standards, spectra were collected for two members of the immunoglobulin supergene family of known 3-dimensional structure, β-2-microglobulin (4) and a murine monoclonal IgG (1). As expected, the spectra of β-2-microglobulin (not shown) and IgG (Fig. 2A) possessed single minima at 215 nm and 217 nm, respectively. The spectra of the two truncated proteins, tICAM(453) and tICAM(185), were similar to each other and to that of ICAM-1 (Fig. 2B, C, and D), with minima at 216 to 217 nm and a broad shoulder at 225 to 230 nm, although the shoulder was more pronounced in tICAM(185) than in tICAM(453). These CD spectra provide additional evidence that the soluble ICAM-1 proteins are properly folded and that they possess significant amounts of β structure.

Inhibition of virus binding by soluble ICAM-1. To compare the effects of the soluble ICAM-1 proteins on virus-receptor binding, a competition binding assay was employed. Various concentrations of soluble competitor ICAM-1 proteins were incubated with ^{35}S-HRV3, and binding to ICAM-1 immobilized on microtiter dishes was determined. As can be seen in Fig. 3A, both truncated forms of ICAM-1 inhibit HRV3 binding at similar concentrations: tICAM(453) and tICAM(185) at concentrations of 3.1 ± 1.8 μM (n = 3) and 9.7 ± 3.2 μM (n = 3), respectively, inhibit the binding of ^{35}S-HRV3 by 50%.

Inhibition of virus infectivity by soluble ICAM-1. The effect of soluble ICAM-1 on rhinovirus infectivity was examined under several different conditions (Fig. 3B and C; Table 1). In the experiment for which the results are shown in Fig. 3B and Table 1 (experiment I), HRV3 was preincubated with various concentrations of soluble ICAM-1, and virus titer was determined by a plaque assay in which soluble ICAM-1 was present during the incubation of the virus with the HeLa cell monolayers. The concentration of tICAM(185) required to reduce infectivity by 50% (IC_{50}) in this experiment was 5.3 μM, similar to the concentration needed to inhibit virus binding by 50%. In contrast, the IC_{50} for infectivity of tICAM(453) was 0.4 μM, eightfold lower than its IC_{50} for

TABLE 1. Neutralization of rhinovirus by soluble ICAM-1

Experiment[a]	Presence of ICAM-1 during:		IC_{50} (μM)[b]	
	Preincubation	Infection	tICAM(185)	tICAM(453)
I	+	+	5.3	0.4
II	+	+	13.2	1.2
III	+		>20	>20

[a] Data for experiment I are shown in Fig. 3B, data for experiment II (high MOI) are shown in Fig. 3C, and data for experiment III are described in the text.

[b] See Materials and Methods for a description of each assay.

virus binding. The IC_{50} for infectivity of tICAM(453) was 13-fold lower than that of tICAM(185). Even though the binding experiments were performed in molar excess of ICAM-1 over receptor binding sites on rhinovirus (the concentration of HRV3 in these experiments was approximately 17 pM, and the concentration of potential receptor binding sites was 60-fold higher, or 1 nM), another infectivity experiment was performed in which the concentration of HRV3 was identical to that in the binding experiments. Consequently, HeLa cells were infected at a high MOI in the presence of soluble ICAM-1 in a single-cycle infection (Fig. 3C and Table 1 [experiment II]). Although the IC_{50} values for tICAM(453) and tICAM(185) are approximately 3-fold higher in the high-MOI experiment than in the plaque assay, the relative difference in the IC_{50} values between the two ICAM-1 species was approximately 11-fold, or essentially the same as in the low-MOI experiment. The difference in absolute IC_{50} values between these two experiments may be due to a nonlinear relationship between infectious particles and infected cells at high MOIs. To determine if the neutralization of HRV3 was reversible, virus was preincubated with soluble ICAM-1 at 20 μM (a concentration known to reduce infectivity >99%; see Fig. 3B), and the mixture was then diluted to negligible ICAM-1 concentrations for infection of HeLa cells. The titers of tICAM(453)- and tICAM(185)-treated virus were 1.9×10^5 PFU/ml and 3.0×10^5 PFU/ml, respectively, compared with 3.6×10^5 PFU/ml for control virus (Table 1, experiment III). Only marginal reduction of virus titer (<50%) was observed at 20 μM soluble ICAM-1, indicating that the ICAM-1-mediated neutralization of rhinovirus is largely reversible; this reversibility is presumably due to simple dissociation of the virus-receptor complex upon dilution.

Thus, the neutralizing activity of tICAM(185) is directly correlated with its ability to inhibit virus-receptor binding, while tICAM(453) neutralizes rhinovirus at a concentration considerably lower than that necessary to inhibit binding and is presumably acting by a mechanism in addition to direct competition for receptor-binding sites on the virus. Neutralization of rhinovirus by both forms of ICAM-1 is largely reversible.

Effect of soluble ICAM-1 on rhinovirus integrity. Samples of ^{35}S-HRV3 incubated with tICAM(453) and tICAM(185) under conditions similar to those in the binding and infectivity experiments were analyzed by sedimentation through sucrose gradients. HRV3 incubated with 10 μM tICAM(453) separated into three peaks, 149S (cosedimenting with native virus), 135S, and 80S (Fig. 4A). The 149S and 135S peaks were infectious, with PFU/cpm ratios of 200 and 267 compared to a value of 200 for native HRV3. The specific infectivity of the 80S species was dramatically reduced to a

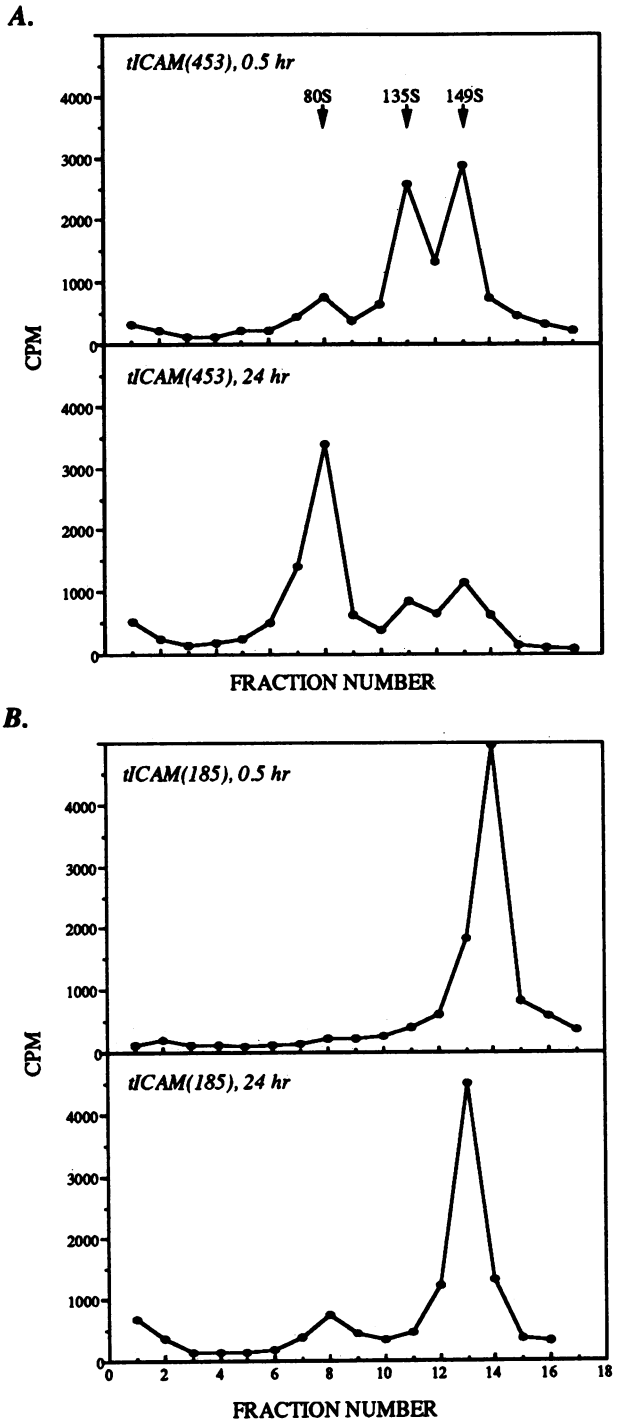

FIG. 4. Sedimentation analysis of HRV3 incubated with soluble ICAM-1. ^{35}S-HRV3 (10^5 cpm) was incubated with 10 μM tICAM (453) (A) or tICAM(185) (B) in N buffer–1 mg of BSA per ml (pH 7.5) for 0.5 and 24 h at 34°C. The mixtures were then sedimented through sucrose gradients as described in Materials and Methods, and the radioactivity in the fractions was determined by scintillation counting. Fractions are numbered from top to bottom of the gradient.

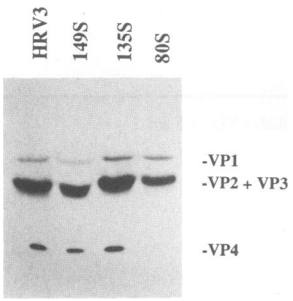

FIG. 5. Capsid protein composition of soluble ICAM-1-modified forms of HRV3. Fractions from control ^{35}S-HRV3 and 149S, 135S, and 80S [from ^{35}S-HRV3 incubated with 10 μM tICAM(453)] were subjected to SDS-PAGE followed by fluorography. Densitometry (normalized to the VP1 band) indicated that the VP4 content of the 80S sample was 9% of control HRV3, 149S, or 135S species.

PFU/cpm ratio of 15; the residual infectivity is probably due to slight contamination from the 149S and 135S peaks since the gradients were fractionated from the bottom. This 80S species was also generated upon incubation with tICAM(185), although less efficiently (Fig. 4B). The fraction of HRV3 in the 80S peak in the sample treated with 10 μM tICAM(453) was 18% after 30 min and 61% after 24 h. The rate of conversion to the 80S species is highly temperature dependent and is greater at 37°C than at 34°C, the optimal temperature for rhinovirus growth (10). Since this concentration of tICAM(453) reduced infectivity to <0.2% (Fig. 3B) and since the reduction of infectivity is largely reversible, the conversion of rhinovirus to the noninfectious 80S species does not play a major role in rhinovirus neutralization by soluble ICAM-1.

The 149S, 135S, and 80S peaks were characterized with respect to their viral capsid composition and RNA content. Analysis of peak fractions by SDS-PAGE revealed that the 149S and 135S peaks possessed all four capsid proteins, while the 80S peak had dramatically reduced amounts of VP4 (Fig. 5). To assess the RNA content of the three peaks, preparations of [^{35}S]methionine- and [^{3}H]uridine-labeled HRV3 incubated with 10 μM tICAM(453) were separated on sucrose gradients (Fig. 6). The radioactivity from the [^{35}S]methionine-labeled virus formed a clear 80S peak, which was insensitive to RNase A. The radioactivity from the [^{3}H]uridine-labeled virus formed 149S and 135S peaks but no 80S peak. When RNase A was included in the incubation, the 149S and 135S peaks were not altered, while the remainder of the radioactivity distributed across the top half of the gradient shifted to the top of the gradient. These data indicate that the 80S peak does not contain RNA and that the 149S, 135S, and 80S peaks are insensitive to RNase A digestion. In a second experiment, the viral RNA content was determined directly by extraction of RNA from equal amounts of radioactivity from 149S, 135S, and 80S peaks of [^{35}S]methionine-labeled HRV3 and then by dot blot analysis with an oligonucleotide probe for the positive (+) strand of rhinovirus (Fig. 7). This experiment showed that the 149S and 135S peaks but not the 80S peak contained viral RNA. Thus, the 80S peak appears to be an empty capsid, lacking both RNA and VP4. The 135S peak contains both VP4 and RNA and is infectious. Although the nature of the 135S peak is unclear at present, it is likely that it is a virion with altered hydrodynamic properties due to interaction with ICAM-1.

DISCUSSION

In this report, we have described the production and characterization of two soluble forms of ICAM-1, the major

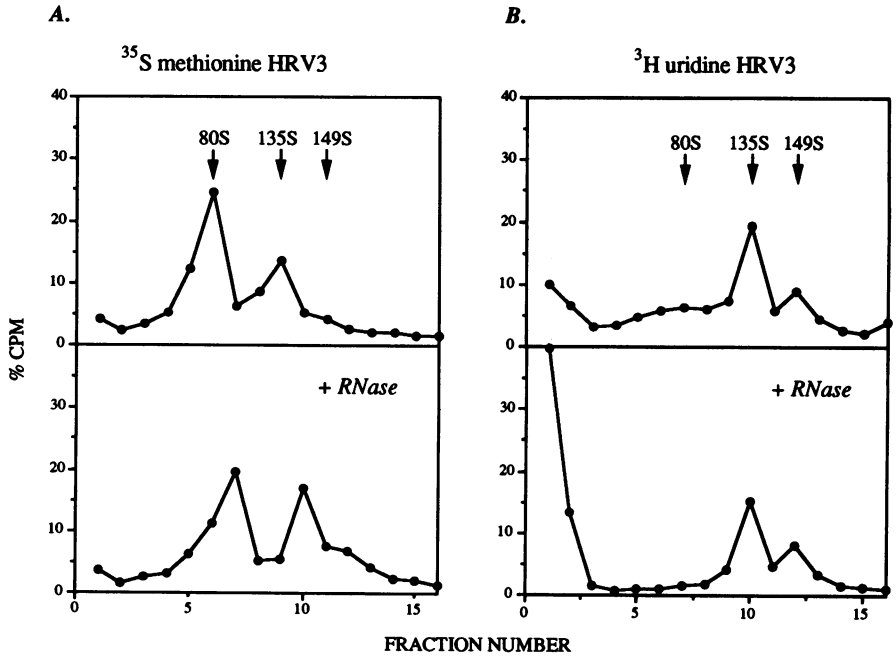

FIG. 6. Viral RNA content of soluble ICAM-1-modified forms of HRV3. Sedimentation analysis of [^{35}S]methionine- (A) and [^{3}H]uridine-labeled (B) HRV3 after incubation with 10 μM tICAM(453) for 30 min at 37°C are shown. Where indicated, RNase A (10 μg/ml) was included in the reaction mixtures. Data are plotted as the percentage of total radioactivity on each gradient (approximately 75,000 cpm and 60,000 cpm for [^{35}S]methionine- and [^{3}H]uridine-labeled HRV3, respectively). Fractions are numbered from top to bottom of the gradient.

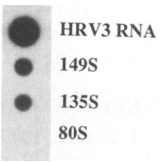

FIG. 7. Detection of viral RNA by hybridization with an oligonucleotide probe. RNA from the 149S, 135S, and 80S peaks of [^{35}S]methionine-labeled HRV3 incubated with tICAM(453) was probed with a ^{32}P-labeled oligonucleotide probe for the positive (+) strand of rhinovirus. The amount of material loaded from each sample was normalized to the amount of [^{35}S]methionine radioactivity extracted, as described in Materials and Methods. HRV3 RNA (50 ng) and RNA from 8 ng (of protein) from the 149S, 135S, and 80S species were applied to the filter.

human rhinovirus receptor, and their effects on virus-receptor binding, virus infectivity, and virus integrity. The results from these experiments allow us to distinguish three distinct mechanisms by which soluble ICAM-1 blocks virus growth and to identify the regions of ICAM-1 responsible for these activities. In addition, the results presented show that receptor protein can uncoat the rhinovirus particle in vitro and, thus, have implications for the mechanism of virus uncoating in vivo.

ICAM-1 has a domain structure that is related to the immunoglobulin supergene family, and its extracellular portion can be divided into five immunoglobulin-like domains (32, 35). Two soluble forms of ICAM-1 have been produced, one corresponding to the entire extracellular domain [tICAM(453); domains 1 through 5] and one corresponding to the two N-terminal immunoglobulin-like domains [tICAM(185); domains 1 and 2]. Constructs coding for domains 1 through 3 were expressed poorly, and domain 1 was not expressed at all in mammalian cells. These data are similar to those obtained with CD4, a related member of the immunoglobulin supergene family (2). A likely explanation for these findings is that an intimate interaction exists between certain domains, particularly between domains 1 and 2, which is required for proper folding or solubility of the polypeptide; the close packing between domains 1 and 2 of CD4 revealed by its crystal structure has provided evidence in favor of this interpretation (28, 37). Physical characterization of tICAM(453) and tICAM(185) indicate that both are asymmetric molecules, consistent with the data of Staunton et al. (34) with regard to a soluble form of ICAM-1 that is essentially the same as tICAM(453). Proteins belonging to the immunoglobulin supergene family would be expected to have domains with the immunoglobulin fold motif, which is basically two apposed sheets of antiparallel β strands with connecting loops (38). CD indicates that both tICAM(453) and tICAM(185) have significant amounts of β structure, consistent with their sequence homologies to immunoglobulin supergene family members, and provides evidence that the proteins are properly folded. However, the CD spectra do have features that are significantly different from those of classical members of the immunoglobulin supergene family; the shoulder at 225 to 230 nm present in the two ICAM-1 species [particularly in tICAM(185)] is not found in the spectra of β-2-microglobulin and IgG. These differences suggest the presence of novel secondary structural features, particularly within domains 1 and 2. Indeed, the homology of many of the domains of ICAM-1 to immunoglobulin supergene family members determined by the ALIGN program (5), while significant, is not high (data not shown). Domain 1, in particular, has a number of unusual features for an immunoglobulin-like domain, such as a relatively short distance (44 residues) between intradomain disulfide bonds and four instead of two cysteines in the B and F β strands. Thus, structural predictions based on the immunoglobulin fold motif should be made with caution.

Competitive binding studies indicate that the binding site for rhinovirus is largely contained within the first two domains. This conclusion is consistent with studies on transmembrane ICAM-1, in that human-mouse chimera studies by Staunton et al. (34) indicate that the rhinovirus binding site is located within domains 1 and 2. Similar studies by McClelland et al. (20) indicate that the rhinovirus binding site is located within domain 1. The reason for the small but significantly (threefold) greater inhibitory activity of tICAM(453) relative to that of tICAM(185) is unclear, although two possibilities are the fact that (i) tICAM(185) is less stably folded than tICAM(453) or (ii) the large size of tICAM(453) creates additional steric interference [relative to tICAM(185)] for a subsaturated virus particle binding to membrane-bound ICAM-1. In studies with transmembrane forms of ICAM-1, Staunton et al. (34) have reported that a shortened form of ICAM-1 containing only domains 1 and 2 binds rhinovirus at approximately 1/10 the level of full-length transmembrane ICAM-1, which they propose is due to inaccessibility to the receptor-binding site on the virus because of the short distance of the virus binding site of ICAM-1 from the plane of the membrane. Direct analysis of the stoichiometry of soluble ICAM-1–virus binding may help to resolve this issue.

The effects of tICAM(453) and tICAM(185) on virus infectivity are clearly distinguishable. tICAM(185) inhibits virus infectivity at essentially the same concentration at which it inhibits virus-receptor binding, indicating that its mode of action is by competitive inhibition of virus binding to cellular receptor. tICAM(453), however, inhibits infectivity at a concentration 10-fold lower than that required for inhibition of binding, indicating a second mechanism for neutralizing virus dependent upon functions encoded by domains 3, 4, and 5. Although the nature of this second mechanism is unclear at present, it is reasonable to conclude that entry or intracellular uncoating steps are involved. One possibility is that the large size of tICAM(453) relative to that of tICAM(185) creates steric problems for subsaturated virus-receptor complexes during the entry or uncoating steps; another possibility is that additional contacts with the virus or with adjacent tICAM(453) molecules on the virion mediated by domains 3, 4, or 5 are responsible for the enhanced neutralizing activity of tICAM(453). Marlin et al. (19) reported a similar disparity between the ability of a soluble ICAM-1 molecule similar to tICAM(453) to inhibit virus-receptor binding and virus infectivity, although this was attributed to differences in the experimental conditions of the two assays. In the binding and infectivity experiments reported here, soluble ICAM-1 is in considerable molar excess above that of virus or viral receptor binding sites and we have performed our binding and infectivity studies at identical rhinovirus concentrations. The results presented here indicate that the differences in the binding and neutralization activities are significant.

Both tICAM(453) and tICAM(185) have the ability to irreversibly inactivate rhinovirus by causing the loss of the viral subunit VP4 and the RNA genome; this constitutes a third mechanism of virus neutralization by soluble receptor. The subviral particles resulting from this alteration are similar in some respects to the eclipse products described for

poliovirus and other picornaviruses generated during infection of cells (7, 8, 13), which are thought to be products of the uncoating process (26). It has been demonstrated that poliovirus can be conformationally altered in cell-free systems by membranes containing poliovirus receptor (6, 12) or detergent-solubilized poliovirus receptor (14) to a 135S form lacking VP4 but still containing RNA (in an RNase-sensitive state). However, release of RNA requires further treatment of the 135S species with high concentrations of salt (14) or SDS (6, 12), and generation of 80S empty capsids requires live cells (8). We have demonstrated here that truncated soluble ICAM-1 can alter rhinovirus to an 80S species lacking both VP4 and RNA and, thus, essentially uncoats the virus. We have also identified an intermediate 135S particle which results from ICAM-1–rhinovirus interaction; this particle differs from the 135S poliovirus altered particle in that it is infectious and contains VP4. These differences between rhinovirus and poliovirus with respect to the products of in vitro virus-receptor interaction may reflect differences in the rate-limiting steps for uncoating between rhinovirus and poliovirus or may reflect the different experimental conditions under which the experiments were performed. The alteration of rhinovirus by soluble ICAM-1 clearly indicates that receptor can completely uncoat rhinovirus in the absence of other cellular components, suggesting that destabilization of the rhinovirus by receptor plays a role in the uncoating process in vivo. This may be a general phenomenon, as it has recently been reported that soluble CD4 induces the release of gp120 from the human immunodeficiency virus virion, and it has been hypothesized that this release of gp120 from virions attached to the cell surface may expose regions of gp41 molecules that could promote fusion of the virion and cell membranes (22, 23), which occurs at neutral pH at the cell surface (36). However, the physiological significance of ICAM-1-mediated uncoating in vivo is unclear since there is also a requirement for a chloroquine-sensitive low-pH step inside the cell for rhinovirus infection (10). A more detailed description of the in vitro alteration of rhinovirus by ICAM-1 and its role in virus uncoating in vivo will be presented elsewhere. However, it is clear from the data presented here that uncoating does not play a major role in soluble ICAM-1-mediated neutralization of rhinovirus under the conditions of optimal rhinovirus growth, since the inhibitory activity of soluble ICAM-1 toward virus infection is largely reversible and because the conversion to the 80S form can only account for a small fraction of this activity.

In conclusion, we have demonstrated that two forms of soluble ICAM-1, tICAM(453) and tICAM(185), inhibit virus-receptor binding and virus infectivity. Differential effects of these two proteins on these processes have defined three distinct mechanisms of virus neutralization. The first mechanism appears to be a simple competition of soluble receptor for receptor binding sites on the virus, and determinants within domains 1 and 2 of ICAM-1 are responsible for this activity. The second mechanism is a reversible neutralization in which virus is apparently blocked at an entry or uncoating step and involves contributions from domains 3, 4, and 5. The third mechanism is an irreversible inactivation of the virus characterized by the loss of the virus subunit VP4 and the RNA genome.

ACKNOWLEDGMENTS

We thank Judy Dziuba for tissue culture and fermentation, Tom Buckholz and Gary Davis for amino acid analysis, Craig Rice and George Mitra (Cutter Laboratories) for fermentation and purification of some of the tICAM(453) used in these studies, Suzy Pafka for photography, David Osterman for instruction and discussions in the use of circular dichroism, Mark Cochran for helpful discussions, and Mike Kamarck for a critical reading of the manuscript.

REFERENCES

1. **Amzel, L. M., and R. J. Poljak.** 1979. Three-dimensional structure of immunoglobulins. Annu. Rev. Biochem. **48**:961–967.
2. **Arthos, J., K. C. Deen, M. A. Chaikin, J. A. Fornwald, G. Sathe, Q. J. Sattentau, P. R. Clapham, R. A. Weiss, J. S. McDougal, C. Pietropaolo, R. Axel, A. Truneh, P. J. Maddon, and R. W. Sweet.** 1989. Identification of the residues in human CD4 critical for the binding of HIV. Cell **57**:469–481.
3. **Bebbington, C. R., and C. C. Hentschel.** 1987. The use of vectors based on gene amplification for the expression of cloned genes in mammalian cells, p. 163–188. *In* D. M. Glover (ed.), DNA cloning—a practical approach, vol. 3. IRL Press, Oxford.
4. **Becker, J. W., and G. N. Reeke.** 1985. Three dimensional structure of β2-microglobulin. Proc. Natl. Acad. Sci. USA **82**:4225–4229.
5. **Dayhoff, M. O., W. C. Barker, and L. T. Hunt.** 1983. Establishing homologies in protein sequences. Methods Enzymol. **91**: 524–545.
6. **DeSena, J., and B. Mandel.** 1977. Studies on the *in vitro* uncoating of poliovirus. II. Characteristics of the membrane-modified particle. Virology **78**:554–566.
7. **Fenwick, M. L., and P. D. Cooper.** 1962. Early interactions between poliovirus and ERK cells: some observations on the nature and significance of rejected particles. Virology **18**:212–223.
8. **Fricks, C. E., and J. M. Hogle.** 1990. Cell-induced conformational change in poliovirus: externalization of the amino terminus of VP1 is responsible for liposome binding. J. Virol. **64**:1934–1945.
9. **Giranda, V. L., M. S. Chapman, and M. G. Rossmann.** 1990. Modeling of the human intercellular adhesion molecule-1, the human major group receptor. Proteins **7**:227–233.
10. **Greve, J. M.** Unpublished data.
11. **Greve, J. M., G. Davis, A. M. Meyer, C. P. Forte, S. C. Yost, C. W. Marlor, M. E. Kamarck, and A. McClelland.** 1989. The major human rhinovirus receptor is ICAM-1. Cell **56**:839–847.
12. **Guttman, N., and D. Baltimore.** 1977. A plasma membrane component able to bind and alter virions of poliovirus type 1: studies on cell-free alteration using a simplified assay. Virology **82**:25–36.
13. **Joklik, W. K., and J. E. Darnell.** 1961. The adsorption and early fate of purified poliovirus in HeLa cells. Virology **13**:439–447.
14. **Kaplan, G., M. S. Freistadt, and V. R. Racaniello.** 1990. Neutralization of poliovirus by cell receptors expressed in insect cells. J. Virol. **64**:4697–4702.
15. **Kim, S., T. J. Smith, M. M. Chapman, M. G. Rossmann, D. C. Pevear, F. J. Dutko, P. J. Felock, G. D. Diana, and M. A. McKinlay.** 1990. Crystal structure of human rhinovirus serotype 1A (HRV1A). J. Mol. Biol. **210**:91–111.
16. **Kingston, R. E.** 1987. Introduction of DNA into mammalian cells, p. 901–906. *In* F. M. Ausubel, R. Brent, R. E. Kingston, D. D. Moore, J. G. Seidman, J. A. Smith, and K. Struhl (ed.), Current protocols in molecular biology. John Wiley & Sons, Inc., New York.
17. **Kishimoto, T. K., R. S. Larson, A. L. Corbi, M. L. Dustin, D. E. Staunton, and T. A. Springer.** 1989. The leukocyte integrins. Adv. Immunol. **46**:149–182.
18. **Marlin, S. D., and T. A. Springer.** 1987. Purified intercellular adhesion molecule-1 (ICAM-1) is a ligand for lymphocyte function-associated antigen (LFA-1). Cell **51**:813–819.
19. **Marlin, S. D., D. E. Staunton, T. A. Springer, C. Stratowa, W. Sommergruber, and V. J. Merluzzi.** 1990. A soluble form of intercellular adhesion molecule-1 inhibits rhinovirus infection. Nature (London) **344**:70–72.
20. **McClelland, A, J. deBear, S. Connonly Yost, A. M. Meyer, C. W. Marlor, and J. M. Greve.** 1991. Identification of monoclonal antibody epitopes and critical residues for rhinovirus binding in domain 1 of ICAM-1. Proc. Natl. Acad. Sci. USA **88**:7993–7997.

21. **Minor, P. D.** 1985. Growth, assay, and purification of picornaviruses, p. 25–40. *In* B. W. J. Mahy (ed.), Virology: a practical approach. IRL Press, Oxford.
22. **Moore, J. P., J. A. McKeating, W. A. Norton, and Q. J. Sattentau.** 1991. Direct measurement of soluble CD4 binding to human immunodeficiency virus type 1 virions: gp120 dissociation and its implications for virus-cell binding and fusion reactions and their neutralization by soluble CD4. J. Virol. **65**:1133–1140.
23. **Moore, J. P., J. A. McKeating, R. Weiss, and Q. J. Sattentau.** 1990. Dissociation of gp120 from HIV-1 virions induced by soluble CD4. Science **250**:1139–1142.
24. **Rossmann, M. G.** 1989. The canyon hypothesis. Hiding the host cell receptor attachment site on a viral surface from immune surveillance. J. Biol. Chem. **264**:14587–14590.
25. **Rossmann, M. G., E. Arnold, J. W. Erikson, E. W. Frankenberger, P. J. Griffith, H. Hecht, J. E. Johnson, G. Kamer, M. Luo, A. G. Mosser, R. R. Rueckert, B. Sherry, and G. Vriend.** 1985. Structure of a common cold virus and functional relationship to other picornaviruses. Nature (London) **317**:145–153.
26. **Rueckert, R. R.** 1990. Picornaviridae and their replication, p. 507–548. *In* B. N. Fields et al. (ed.). Virology. Raven Press, New York.
27. **Rueckert, R. R., and M. A. Pallansch.** 1981. Preparation and characterization of encephalomyocarditis (EMC) virus. Methods Enzymol. **78**:315–326.
28. **Ryu, S., P. D. Kwong, A. Truneh, T. G. Porter, J. Arthos, M. Rosenberg, X. Dai, N. Xuong, R. Axel, R. W. Sweet, and W. A. Hendrickson.** 1990. Crystal structure of an HIV-binding recombinant fragment of human CD4. Nature (London) **348**:419–426.
29. **Saiki, R. K., S. Scharf, F. Faloona, K. B. Mullis, G. T. Horn, H. A. Erlich, and N. Arnheim.** 1988. Primer-directed enzymatic amplification of DNA with a thermostable DNA polymerase. Science **239**:487–491.
30. **Sambrook, J., E. F. Fritsch, and T. Maniatis.** 1989. Molecular cloning, a laboratory manual. Cold Spring Laboratory Press, Cold Spring Harbor, N.Y.
31. **Seed, B.** 1987. An LFA-3 cDNA encodes a phospholipid-linked membrane protein homologous to its receptor CD2. Nature (London) **239**:840–842.
32. **Simmons, D., M. W. Makgoba, and B. Seed.** 1988. ICAM, an adhesion ligand of LFA-1, is homologous to the neural cell adhesion molecule NCAM. Nature (London) **331**:624–627.
33. **Springer, T. A.** 1990. Adhesion receptors of the immune system. Nature (London) **346**:425–434.
34. **Staunton, D. E., M. L. Dustin, H. P. Erickson, and T. A. Springer.** 1990. The arrangement of the immunoglobulin-like domains of ICAM-1 and the binding sites for LFA-1 and rhinovirus. Cell **61**:243–254.
35. **Staunton, D. E., S. D. Marlin, C. Stratowa, M. L. Dustin, and T. A. Springer.** 1988. Primary structure of intercellular adhesion molecule 1 (ICAM-1) demonstrates interaction between the immunoglobulin and integrin supergene families. Cell **52**:925–933.
36. **Stein, B. S., S. D. Gowda, J. D. Lifson, R. C. Penhallow, K. G. Bensch, and E. G. Engleman.** 1987. pH-independent HIV entry into CD4-positive T cells via virus envelope fusion to the plasma membrane. Cell **49**:659–668.
37. **Wang, J., Y. Yan, T. P. J. Garrett, J. Liu, D. W. Rodgers, R. L. Garlick, G. E. Tarr, Y. Husain, E. L. Rheinherz, and S. C. Harrison.** 1990. Atomic structure of a fragment of human CD4 containing two immunoglobulin-like domains. Nature (London) **348**:411–418.
38. **Williams, A. F., and A. N. Barclay.** 1988. The immunoglobulin superfamily-domains for cell surface recognition. Annu. Rev. Immunol. **6**:381–405.